

# Spectrometer for Laser-Driven Plasma Wakefield Accelerator

by

Michael E. Garbus

Virginia Polytechnic Institute and State University  
Hampton University (UnIPhy-REU)

July 27, 2000

Mentor:

Dr. Paul Guèye

Hampton University

TJNAF

## Abstract

A spectrometer beam-line for the Laser-driven plasma wake field electron beam (technique developed at the University of Michigan) has been developed at Hampton University. In this non-conventional technique, the electron beam is created and accelerated up to a few GeV/cm when a high power laser beam (few Tera Watts in hundreds of Femto seconds) is impinged on a helium gas jet. Results from an experiment performed in 1997 revealed that (a) the momentum spectrum peaked around 7 MeV/c with an exponential fall-off at high momenta up to  $(70.3 \pm 19.9)$  MeV/c and (b) the number of electrons detected per beam were  $(5.5 \pm 0.6) \times 10^8$ . Recent upgrades in the laser led to this new design. An experiment is being currently conducted to determine with a much better accuracy (almost an order of magnitude) the characteristics of this electron beam (shape, distribution, profile, current...) for future nuclear and particle physics applications.

# 1 Introduction

Man has yet to fully understand the universe in which he lives. Mankind is currently trying to better understand the tiny fundamental particles and their behavior when they interact with each other in branches of science called nuclear and particle physics. Nuclear physics has evolved greatly with the aid of tools, such as laboratories like CERN and TJNAF, for exploring subatomic matter. These laboratories use matter moving at extremely high speeds to probe the inner works of matter. At TJNAF, a stream of electrons, moving near the speed of light, with a maximum energy of  $4\text{GeV}$  is used to investigate subatomic matter. Tools like these have acquired great accuracy and have given scientists more options as technology has evolved. But the complexity and size of these exploratory tools has grown as well.

At the University of Michigan, the NSF's Center for Ultrafast Optical Science (CUOS) has developed a technique that uses two table-sized lasers to produce a burst of high energy electrons. There are many benefits to perfecting this new wake field acceleration technology. For instance it is extremely cheap to build and maintain relative to laboratories such as TJNAF and CERN. It cost over \$600 million to build TJNAF, and the DOE alone allotted over \$70 million for running and maintaining TJNAF for 1999. It is estimated that to build and maintain the table-sized plasma wake field electron accelerator, it would only cost a few million dollars annually. This means that universities and countries with relatively small budgets would be able to perform cutting-edge physics research. Nuclear and particle physics will no longer be performed only by large organizations.

## 2 Wake Field Acceleration

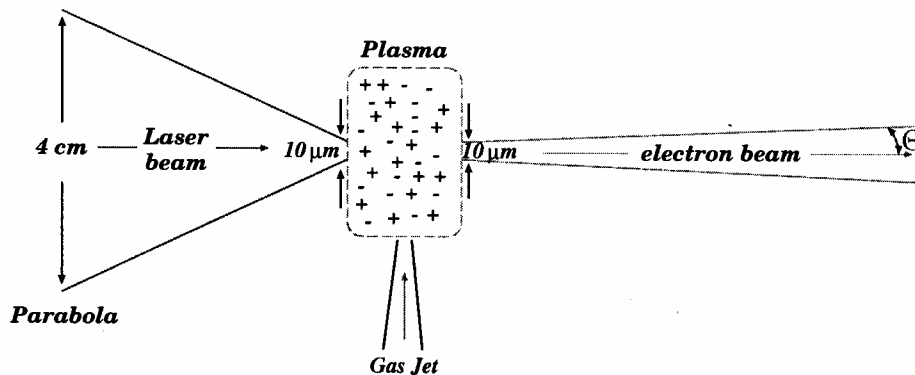


Figure 1: Laser interaction with gas jet to create wake field acceleration.

The electrons are produced and accelerated using laser-driven wake field electron acceleration. This was employed at the Center for Ultrafast Optical Science using a technique called *chirped pulse amplification* which produces a laser pulse with a

duration of 400 fs and a maximum energy of 2 J. The laser has a peak power of 5 TW with electromagnetic intensities exceeding  $3 \times 10^{18} \text{ W/cm}^2$ . The laser is then impinged on a helium or argon gas jet. From this interaction, a plasma is created by tunneling ionization and exciting an electron plasma wave through Raman forward scattering. The extremely high laser pressure, ponderomotive force, pushes the atomic electrons of the gas out of the way, creating a plasma. The more massive positive ions attract the dispersed electrons back due to the Coulomb force. This sets up a plasma in the wake of the laser pulse. This setup is shown in Fig. 1. The plasma wave effectively rectifies the laser's electromagnetic field so that it becomes an electrostatic field propagating in the laser pulse direction at close to the speed of light. Plasma electrons encountering this field may be accelerated up to near a few GeV or more.

In a preliminary experiment conducted in 1997, the measured peak momentum spectrum was about  $7 \text{ MeV}/c$  with an experimental fall-off at high momenta up to  $(70.3 \pm 19.9) \text{ MeV}/c$ . There were about  $(5.5 \pm 0.6) \times 10^8$  electrons measured in each burst. In order to perform an experiment in particle physics, electrons traveling with energies greater than  $300 \text{ MeV}$  are necessary. In theory, an increase in the electron plasma density and increasing the power of the laser will yield an increase in the mean energy of electrons. This relationship is expressed in the following equation:

$$P_c[\text{GW}] = 17 \left( \frac{\sigma_o^2}{\sigma_p^2} \right) \quad (1)$$

where:

$\sigma_o$  = laser frequency

$\sigma_p = \sqrt{n_e e^2 / m \epsilon_o \gamma}$

$m$  = electron mass

$n_e$  = plasma electron density

$\gamma = \sqrt{1 + a_o^2/2}$  is relativistic factor for a linearly polarized laser

$a_o = 8.5 \times 10^{-10} \lambda [\mu\text{m}] x I^{1/2} [\text{W/cm}^2]$

## 3 Spectrometer Design

### 3.1 Goals

The new beam line should be able to allow us to: (i) extract the beam's characteristics (profile, current, momentum . . .), and (ii) investigate the possibility for nuclear physics experiments. In the present document, we will focus only on the beam line.

The design of the beam line is based on the following assumptions:

1. **Incident beam energy:** 200 MeV
2. **Original beam spot size:** 10  $\mu\text{m}$
3. **Original beam divergence angle:**  $2^\circ$
4. **Maximum distance gas jet to first quadrupole (Q1):** 20 cm

## 5. Inside diameter of the beam pipe: 5.08 cm

The proposed QQQDD beam line is shown in Fig. 2. We stress that this design is very dependent on the beam's characteristics: this beam line will not work if the given assumptions for the original beam properties are not satisfied. In 1997, we detected about  $10^9$  electrons out of the  $10^{11}$  potentially produced. This result is mainly due to the emittance of the beam ( $0.6\pi$  mm.mrad) which caused an important loss in the number of electrons from their point of production (at the laser-gas jet interaction point) to the location of our fiber arrays (item 13 on Fig. 3). We shall see in the following sections that with the expected improved beam emittance and the beamline design, we are able to maintain the beam envelope within a 5.08 cm inside diameter beam pipe, and thus collect all the (accelerated) produced electrons.

The optical and magnet specifications are reviewed in section 3.2 and 3.3. The beam pipe is described in section 3.4. The methods that will be used to extract the beam's properties will be discussed in section 3.5.

## 3.2 Optics

The optimization of the magnet requirements – mainly the magnetic fields, the physical lengths and the distances between elements – have first been investigated by the means of two beam transport codes: TRANSPORT and OPTIM. These two programs have been especially built to design beam transport systems. While TRANSPORT is a FORTRAN based programming language code, OPTIM has been developed in C++. They are identical but offer different advantages. Both of them provide various information on the beam while transporting through the beam line: magnetic fields, magnet lengths, transfer matrices, momentum, spatial and angular dispersions, magnet alignments, ...

The results obtained from both programs for a 200 MeV incident electron beam energy are shown in Fig. 4 and 5. The trajectories shown are radial trajectories. In TRANSPORT, the horizontal-X and vertical-Y curves correspond to the size of the beam envelope inside the beam pipe. In OPTIM,  $Ax\_bet$  and  $Ay\_bet$  correspond to the position of the beam's center of gravity inside the beam pipe; and  $Ax\_disp$  and  $Ay\_disp$  (always equals to zero) represent the beam dispersions with respect to the central trajectory. The X-horizontal and Y-vertical displacements of the beam along the beam line obtained from both codes are compared in Table 1. One can see that (as expected) both codes give the same results<sup>1</sup>.

## 3.3 Magnet specifications

The optics discussed in the previous section use the three quadrupoles and two dipole magnets specifications listed in Tables 2 and 3: (i) a 5.08 cm beam pipe diameter, (ii) two identical 10 cm long quadrupoles with a maximum field tip of 3 kG at the

---

<sup>1</sup>The differences obtained (less than 3 mm) are due to the fact that while TRANSPORT gives an output of the (X,Y) values, OPTIM does not. One has to *click* on the picture to extract them. Therefore, the accuracy of the values obtained is user dependent.

	Field	Length	X-Horizontal	Y-vertical
<b><u>OPTIM</u></b>				
Q1	2.965 kG/cm	10 cm	0.92 cm	1.34 cm
Q2	-2.89 kG/cm	15 cm	1.29 cm	2.09 cm
Q3	2.59 kG/cm	10 cm	2.13 cm	1.32 cm
D1	2.000 kG	50 cm	1.34 cm	1.10 cm
D2	6.986 kG	50 cm	1.83 cm	0.35 cm
<b><u>TRANSPORT</u></b>				
Q1	2.965 kG/cm	10 cm	0.88 cm	1.24 cm
Q2	-2.89 kG/cm	15 cm	1.30 cm	1.99 cm
Q3	2.59 kG/cm	10 cm	2.06 cm	1.18 cm
D1	2.000 kG	50 cm	1.30 cm	0.64 cm
D2	6.986 kG	50 cm	1.78 cm	0.33 cm

Table 1: Comparison of the X-horizontal and Y-vertical beam displacements inside the beam pipe obtained from OPTIM and TRANSPORT codes.

pole, (iii) one 15 cm long quadrupole with a maximum field tip of 3 kG at the pole, (iv) a 50 cm long dipole magnet with a maximum field of 2 kG.m which can bend a 200 MeV electron beam to a 20° angle, and (v) a 50 cm long dipole magnet with a maximum field of 3.49 kG.m which can bend a 200 MeV electron beam to a 30° angle.

	Q1-Q3	Q2
<b>Effective length</b>	10 cm	15 cm
<b>Maximum Pole Tip Field</b>	0.3 Tesla	0.8 Tesla
<b>Maximum Gradient</b>	11.8 T/m	11.8 T/m
<b>Aperture Diameter</b>	5.08 cm	5.08 cm
<b>Pole Profile</b>	Facetted	Facetted
<b>Yoke Shape</b>	Square	Square
<b>Total Weight</b>	37 kg	55 kG
<b>Power Supply</b>	50A/10V	50A/10V

Table 2: The specifications of the three quadrupoles.

In anticipation of an increase in the beam energy, we have investigated the ability of our beam line and change the dipole effective length from 3.49 kG.m to 10 kG.m which can bend a 570 MeV beam to 30°. Assuming a 400 MeV incident beam with the same original conditions as the 200 MeV (listed in section 3.1), the different options to transport such beam are:

	D1	D2
<b>Effective length</b>	50 cm	50 cm
<b>Maximum Field</b>	0.2 Tesla	1 Tesla
<b>Bending angle</b>	2°	30°
<b>Bending Radius</b>	14.3 mm	955 mm
<b>Pole gap</b>	5.08 cm	5.08 cm
<b>Width gap</b>	20.0 cm	22.0 cm
<b>Pole Profile - Entrance/Exit</b>	Approx. Rogowski	Approx. Rogowski
<b>Pole Profile - Sides</b>	Sharp edge	Sharp edge
<b>Total Weight</b>	360 kg	1000 kG
<b>Power Supply</b>	50A/10V	240A/40V

Table 3: The specifications of the two dipole magnets.

- Decrease the beam emittance: either with a new optic (laser-gas jet interaction) or by inserting a collimator between the production source and the first quadrupole (Q1);
- Increase the field tip at the pole for the quadrupoles: this will require to either increase the length of the quadrupoles or the field itself. In any case, the cost of such magnet will be expensive;
- Increase the diameter of the beam pipe: at least a diameter of about 10.16 cm will be needed. But the corresponding budget will increase drastically compared to the one for a 5.08 cm. The reason is simple: an increase in the beam pipe diameter corresponds to an increase in the same amount of the gradient of the magnets in order to keep the same focusing power. In other words, not only the magnets will be heavier but also far more expensive;
- Increase the length of the beam line: using the same magnets, the entire length of the beam line will be approximately doubled (from 2.4 m to about 5-6 m). Study of the corresponding optics has not been investigated.

All the magnets will be running in a DC configuration. Because of the required input current for the 10k G.m dipole magnet, it will also be water cooled. A fourth quadrupole magnet will be purchased as a spare for the other three quadrupoles (3 kG at the pole, 10 cm long).

### 3.4 Beam pipe

From section 3.2, one can notice that the beam envelope is lower than 2.5 cm (in radius) from its point of production (at the laser-gas jet interaction) to the end of the dipole magnet. Therefore, a beam pipe with a 5.08 cm inside diameter should be sufficient. Compare to 1997, no collimator in front of the vacuum chamber is

necessary for an energy less than 200 MeV: the entire electron beam can now be transported without major losses.

While in 1997 the vacuum inside the beam pipe was about  $10^{-1}$  Torr, we have incorporated the use of a vacuum pump (E2M30 double stage) which will be able to give a vacuum on the order of  $10^{-4}$  Torr. This low vacuum and the small length of the entire beam pipe (about 3 to 4 meters) allow the possibility to use simple compress seals instead of standard flanges (which will decrease the cost of the beam pipe). To prevent back-migration of rotary pump oil into the system, a fore-line trap (FL20K) will be added (see table 4). The purpose of this pump is to decrease the spread of the beam due to multiple scattering.

<b>Pump Type</b>	E2M30 double stage
<b>Pumping speed</b>	650 l/min
<b>Vacuum</b>	$0.75 \times 10^{-5} - 3.75 \times 10^{-3}$ Torr
<b>Inlet connection</b>	NW25 flange
<b>Outlet connection</b>	nozzle 15 mm external diameter
<b>Trap type</b>	Fore-line model FL20K

Table 4: The specifications of the vacuum pump.

The alignment of the different elements of this beam line was performed on a bench at Jefferson Lab. Precise offsets (with respect to the beam ideal trajectory) of each element will be measured by the use of teodolytes and recorded as fiducial marks on the beam pipe itself. The position of the entire system at CUOS was performed with relative measurements.

### 3.5 Beam properties

To extract the beam properties, we will use the same data acquisition that was especially developed for the 1997 experiment. Minor modifications will be applied to suit the beam line design.

#### 3.5.1 Beam position and beam profile

The beam position will be monitored by the means of several (fluorescent) BeO viewers which can be inserted inside the beam pipe and a set of fiber arrays. For each viewer, a CCD camera may be added to allow the users to see the beam. The beam horizontal and vertical profiles will be extracted using an array of plastic scintillating fibers coupled to a position sensitive photo-multiplier tube (PMT). The same sixteen input/output Hamamatsu H6568 PMTs will be used. However, due to the expected higher signal (1,000 times bigger), the 3 mm thick fibers will be replaced by 1 mm thick fibers to decrease the pick-up signal and avoid overflows in the Analog-to-Digital Converter (ADC) cards. The option of adding optical attenuators will also be available if the signals bring the PMTs to saturation.

### 3.5.2 Beam momentum and momentum spread

By varying the dipole field strength and placing the fiber arrays immediately after the dipole, the beam momentum spread will be extracted by looking at the position of the outgoing electrons. Assuming the beam propagating along the Z-axis, the dispersion along the horizontal X-axis and Y such that (X,Y,Z) is a direct coordinate system, these parameters are related via:

$$X = -\frac{e \int Bdl}{2P_0 \cos^2 \theta_0} Z^2 + \tan \theta_0 Z + X_0, \quad (2)$$

where:  $e$  is the charge of the electron,  $\int Bdl$  the total magnetic field of the dipole,  $P_0$  the beam momentum,  $\theta_0$  the original beam divergence angle and  $X_0$  the original beam position at the entrance of the dipole magnet.  $\int Bdl$  is obtained by mapping the dipole magnet and looking at the curve  $\int Bdl = f(I_{set})$  which gives the relation between the magnetic field and the setting current of the dipole.

By measuring  $X$  with the fiber arrays, the momentum  $P_0$  can then be extracted. The uncertainty  $\Delta X$  on the position is defined by the width of the fibers (1 mm). Consequently, the uncertainty on the beam momentum  $\Delta P_0$  depends on both  $\Delta X$  and the aperture of the movable slit which will be placed after the dipole and used as a collimator.

### 3.5.3 Beam current

Integrating the signals obtained from all the fibers, the total number of electrons can be evaluated. As a redundant measurement of the beam current, we will also place a Faraday cup at the end of the beam line (see Fig. 6). By shielding appropriately the cup, a noise level less than about 200 mV can be achieved.

## 4 Acknowledgements

This paper was produced during the author's participation in the UnIPhy-REU program at Hampton University, which was funded and made possible by the National Science Foundation (NSF grant number 9988037). I would like to personally thank Dr. Paul Guèye, my mentor, for volunteering to educate a person such as myself, but most of all for his friendship. I would also like to thank Dr. Claudia Rankins and my fellow peers in the UnIPhy program. Thank you Hampton University, University of Michigan, and TJNAF for supporting my education through the use of your materials and equipment.

## 5 Works Cited

### References

- [1] K. A. Assamagan et al., *Electron Beam Characteristics of a Laser-Driven Plasma Wakefield Accelerator*, submitted to NIM, (1998).



- [2] D. Umstadter et al., *Nonlinear Optics in Relativistic Plasmas and Laser Wake Field Acceleration of Electrons*, Science, **273**, 472-475, (1996).
- [3] D. Umstadter *Terawatt Lasers Produce Faster Electron Acceleration*, Laser Focus World, 101-107 (1996).
- [4] D. G. Carey, K. L. Brown and F. Rothacker, *Third-Order Transport, A Computer Program For Designing Charged Particles Beam Transport Systems*, SLAC-R-95-462, (1995).
- [5] V. Lebedev, *OPTIM Reference Manual*, private communication, Jefferson Lab, (1998)
- [6] *GEANT Detector and Simulation Tool*, CERN Geneva, (1994).
- [7] X. Wang et al. *Electron Acceleration and the Propagation of Ultrashort High-Intensity Laser Pulses in Plasmas*, Physical Review Letters, 5324-5327 (2000).

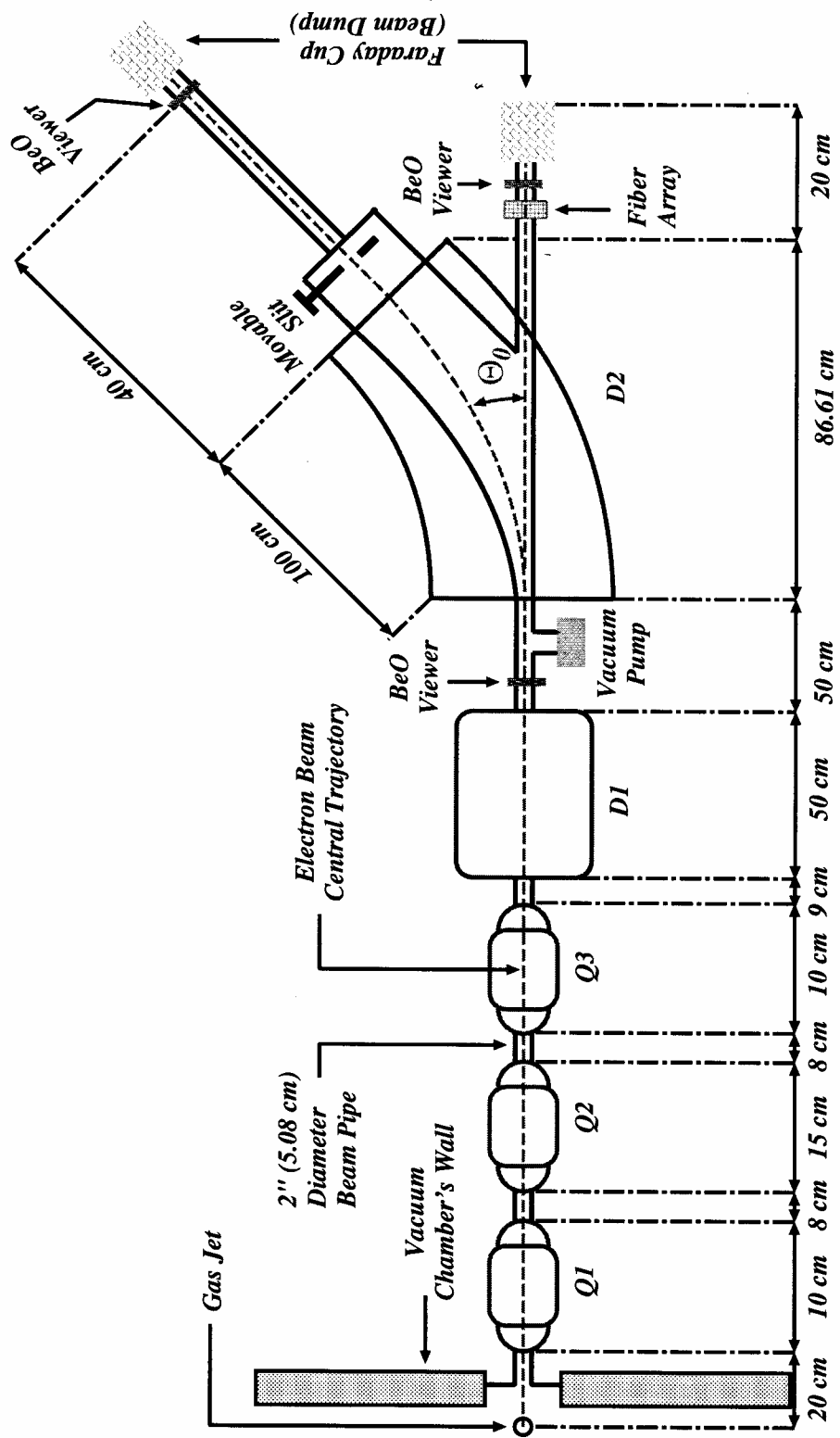


Figure 2: The proposed experimental beam line as of November 1998.

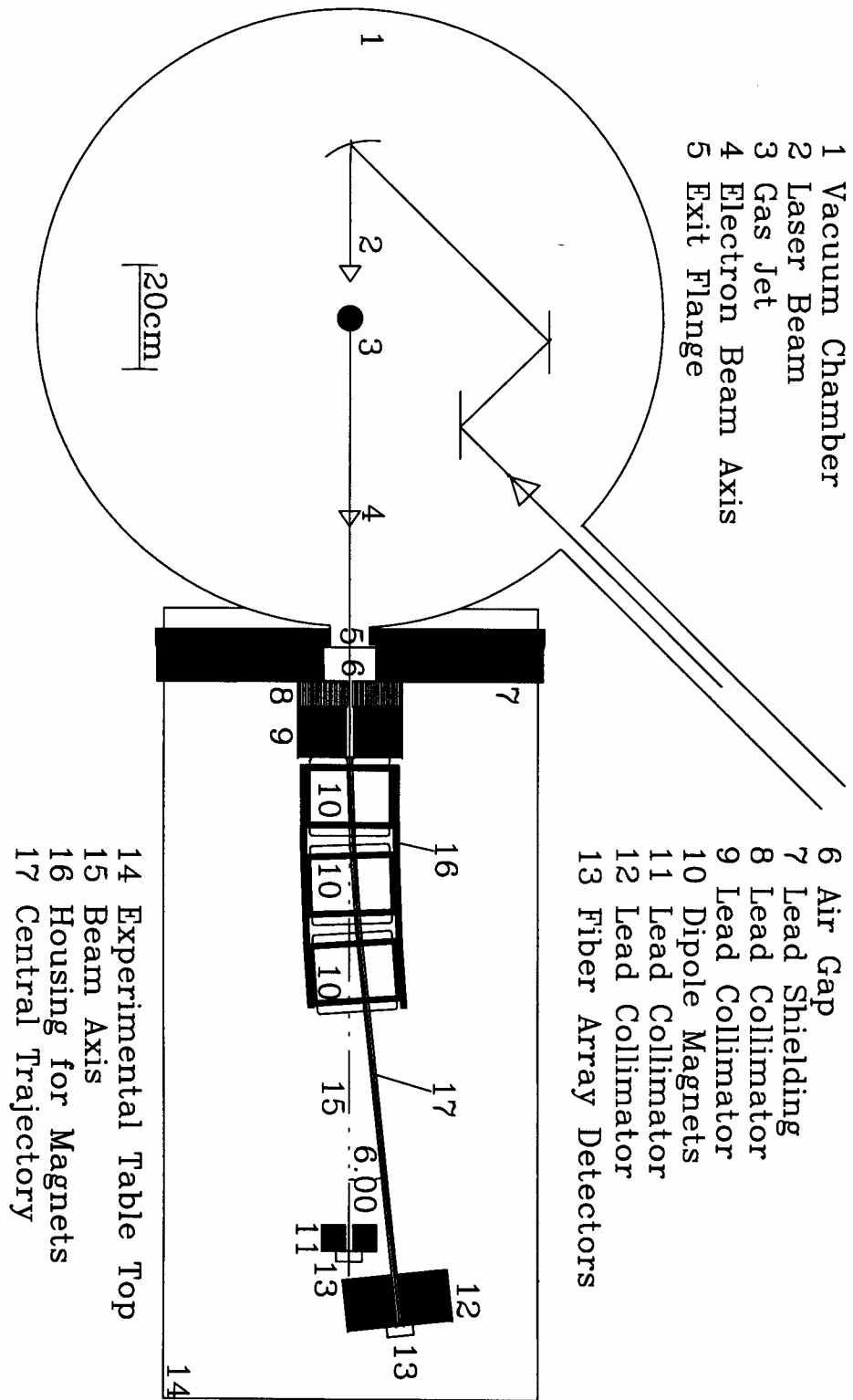


Figure 3: The experimental beamline used during the experiment conducted in 1997.

Michigan-Hampton Wake Field Accelerator Beam Line - TRANSPORT - 200 MEV

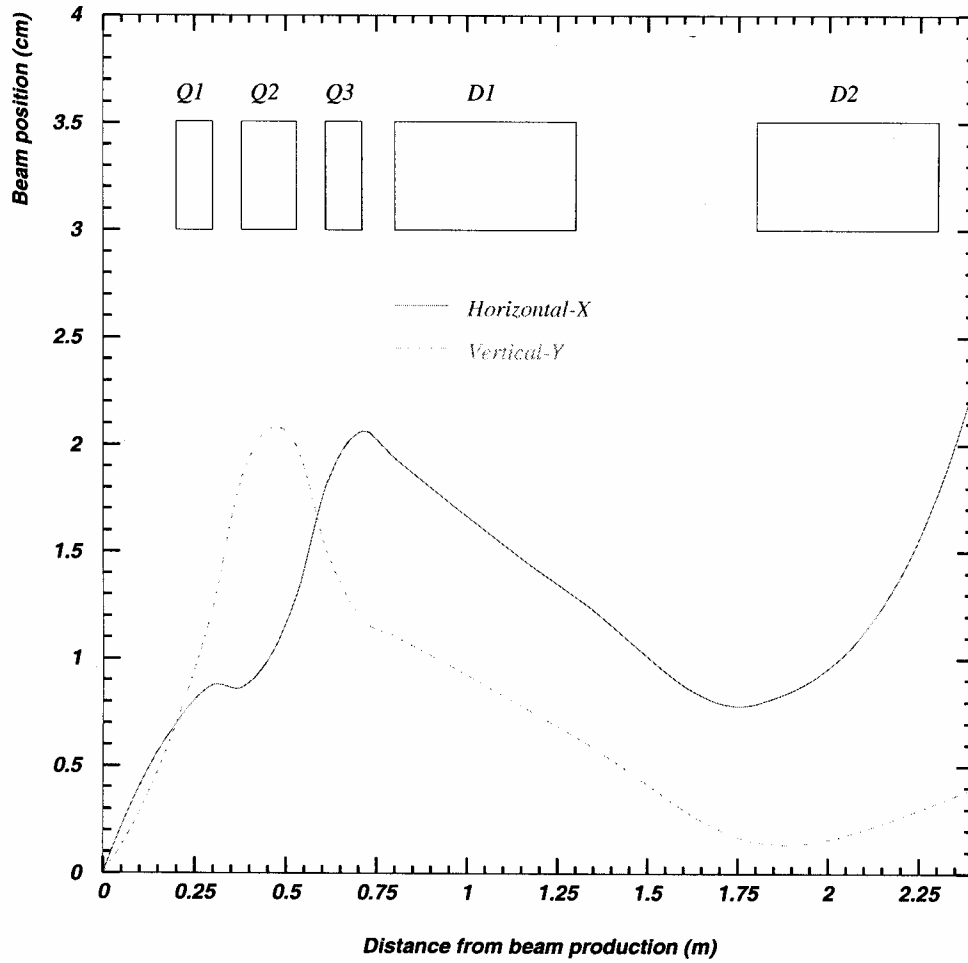


Figure 4: The optimized beam line from TRANSPORT for a 400 MeV incident beam.

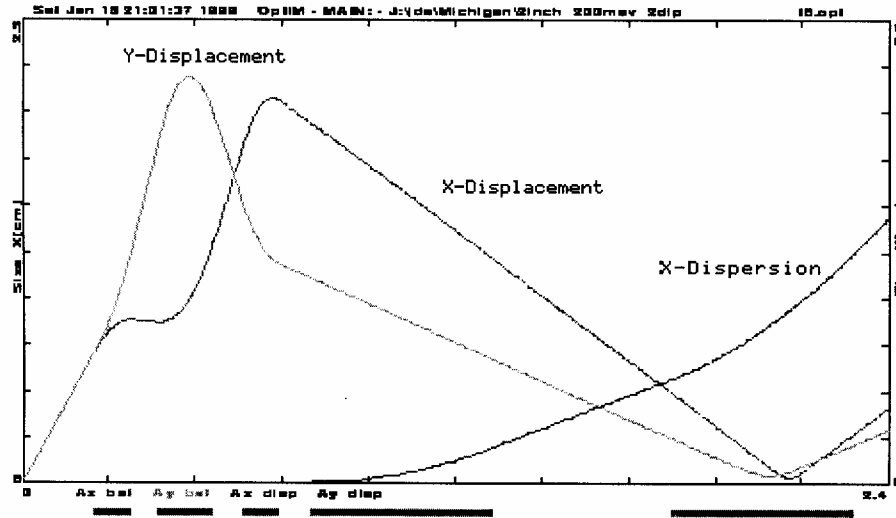


Figure 5: The optimized beam line from OPTIM for a 200 MeV incident beam.

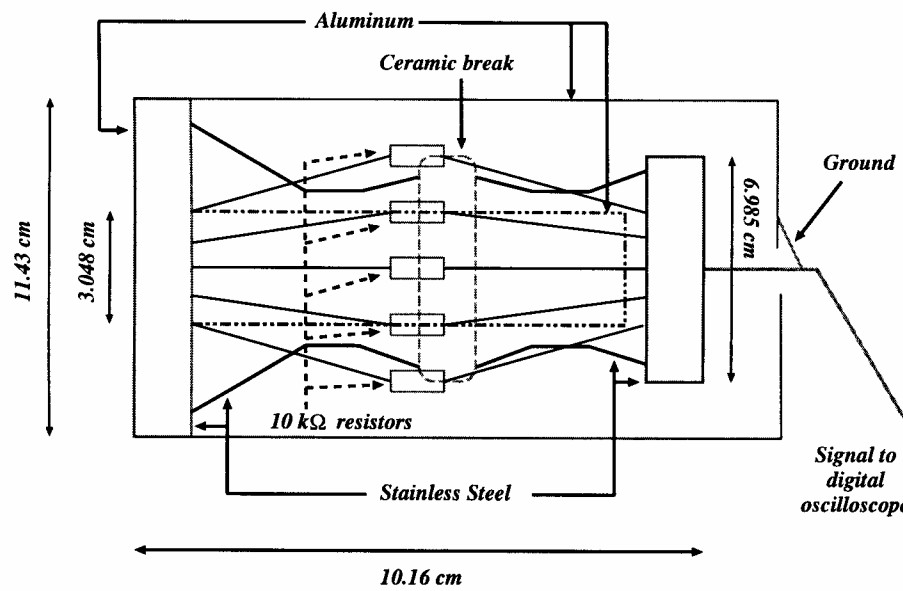


Figure 6: The Faraday cup.